Beauty production and $F_2^{b\bar{b}}$ at HERA

Massimo Corradi[a] (on behalf of the H1 and ZEUS collaborations)

[a]INFN Bologna, via Irnerio 46, Bologna (`massimo.corradi@bo.infn.it`)

The status of beauty measurements at HERA is reviewed. A considerable improvement in the precision and kinematic coverage has been achieved in the last years. The results are in good agreement with NLO QCD.

1. Introduction

QCD calculations for the production of beauty at HERA have relatively small uncertainties, thanks to the large b quark mass, m_b. Moreover, the production cross section for heavy quarks (HQ) is roughly proportional to the gluon content of the proton and could provide, in principle, a stringent constraint to the gluon parton density function (PDF). The main problem is of an experimental nature: measuring beauty at HERA is not simple due to its small cross section. For this reason a big effort has been devoted in the last years by the two HERA collaborations, H1 and ZEUS, to improve the precision of their measurements.

A short review of the status of beauty measurements at HERA will be given here, starting with a summary of the theoretical framework from an experimentalist point of view in Sec. 2, and a short description of the experimental methods in Sec. 3. The photoproduction results are summarized in Sec. 4, while Sec. 5 gives an introduction to the beauty structure function $F_2^{b\bar{b}}$, and in Sec. 6 the deep inelastic scattering (DIS) measurements are presented.

2. Theoretical framework

2.1. QCD calculations

At leading order (LO) in α_S, b quarks are produced in ep collisions through the boson–gluon–fusion (BGF) process of Fig. 1(a). Due to the photon propagator, the cross section is dominated by the region with small four-momentum transfer $Q^2 \sim 0$. In this region the ep collision can be seen

as an interaction between a real photon, emitted from the electron, and the proton (photoproduction) and can be calculated in the Weizsäcker-Williams (WW) approximation [1]. Resolved photon processes, in which the photon behaves as a source of partons (Fig. 1(b)) should give a significant contribution to the photoproduction cross section but are expected to be suppressed at large Q^2.

Next-to-leading order (NLO) corrections ($\mathcal{O}(\alpha_s^2)$) for HQ production in ep collisions are known since the '90s and are available in the form of two programs that allow the calculation of cross sections with arbitrary cuts on the final state: FMNR [2] for photoproduction (it uses the WW approximation and includes resolved–photon processes) and HVQDIS [3] for the DIS (i.e. high-Q^2) regime.

The NLO corrections are significant, with K factors $\sigma^{\mathrm{NLO}}/\sigma^{\mathrm{LO}} \sim 1.4$. In particular a large contribution comes from NLO diagrams of the type shown in Fig. 1(c) that can be seen as a "flavour–excitation" (FE) process in which the photon fluctuates into a $b\bar{b}$ pair, and the b quark of which interacts with a parton from the proton. FE processes are sometimes included also in LO Monte Carlo (MC) programs such as Pythia [4].

Fixed–order calculations may be of limited precision in particular regions of phase space where resummation of large logarithms may be needed: the high-p_T region ($p_T \gg m_b$), the small-x region and the large Q^2 region ($Q^2 \gg m_b^2$). While these effects are relevant for charm production at HERA and for beauty production at the Tevatron or at the LHC, they are expected to be small for
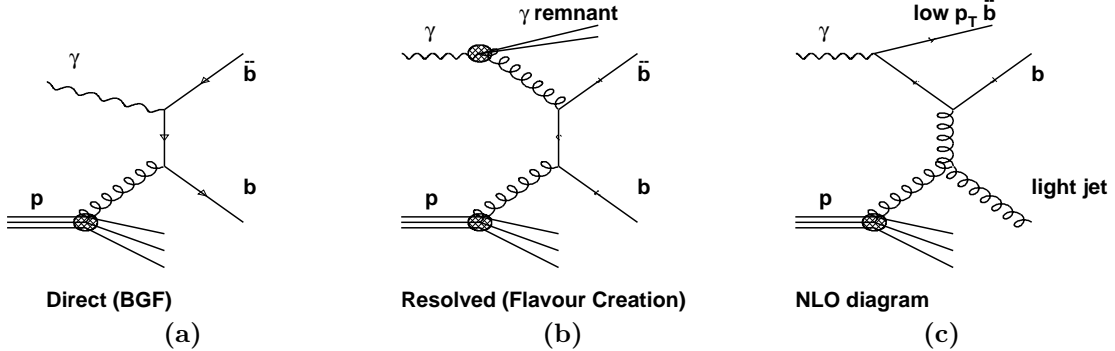
Figure 1. Diagrams contributing to beauty production

the production of beauty at HERA, since m_b^2 is always comparable with the other scales involved in the process (p_T^2, Q^2). This is confirmed by the agreement [5] of fixed-order NLO results with calculations that include large p_T^b resummation [6], large Q^2 resummation [7], and with calculations performed in the k_T factorisation approach [8] that include low-x effects. Threshold corrections ($\hat{s} \sim 4m_b^2$), which are currently only available for hadroproduction [9], may be relevant for b at HERA but are anyhow expected to be within the scale uncertainty of NLO calculations.

2.2. Theoretical uncertainties

The theoretical uncertainties on the NLO predictions can be evaluated by varying the parameters used in the calculation. The uncertainties on the photoproduction cross section, evaluated using FMNR [5], are $\sim 30\%$ from the variation of m_b in the range $m_b = 4.75 \pm 0.25$ GeV and $\sim 20\%$ from the variation of the renormalisation and factorisation scales in the range $\mu_r = \mu_f = 2^{0\pm1} m_T$, where $m_T^2 = m_b^2 + \frac{1}{2}[(p_T^b)^2 + (p_T^{\bar{b}})^2]$. In DIS the uncertainties are smaller: $\sim 15\%$ from the variation of m_b and $\sim 10\%$ from the scale variation as evaluated using HVQDIS [10].

The uncertainty coming from the PDFs (mainly the gluon in the proton) is $\sim 3\%$ ($\sim 6\%$) according to the MRST2001E (CTEQ6.6) PDF sets.

In particular corners of the phase space, dominated by three jets configurations, the $\mathcal{O}(\alpha_s^2)$ calculations are effectively leading order and therefore less precise. These corners include the region of small azimuthal separation between the two highest-p_T jets $\Delta\Phi^{jj}$ and the region of small x_γ^{jets}, where x_γ^{jets} is the fraction of the photon $E - P_Z$ carried by the two highest-p_T jets in the laboratory frame: $x_\gamma^{\text{jets}} = (\sum_{j=1,2} E^j - P_Z^j)/(2y)$.

2.3. Non–perturbative effects

Experiments do not measure b quarks directly but rather B hadrons, leptons from B decays or jets containing B hadrons. The perturbative calculations should therefore be interfaced with models of hadronisation (and decay) to be compared with experimental data. The B hadron spectrum is obtained by folding the quark distributions with phenomenological fragmentation functions based on available experimental data from e^+e^- collisions at the Z^0 pole [11]. The main effect of fragmentation is to produce B hadrons with a p_T distribution softer than that of b quarks by $\Delta p_T/p_T = \mathcal{O}(\Lambda^{\text{QCD}}/m_b)$, which is a small effect for beauty (but not for charm).

Observables that involve the presence of jets require an additional correction for jet hadronisation effects. This is typically obtained using MC models. The corresponding uncertainty is estimated by comparing different models. It can be minimised using an appropriate jet definition, for example k_T jets in which the weakly decaying B hadrons are considered as stable particles, using the E recombination scheme (jet four-momentum given by the sum of particle four-momenta). In this case the jet hadronisation uncertainties are around 5%.

In the case of leptonic observables, the momen-

tum distribution of the lepton from B decays is taken from precise measurements performed at the B factories.

Overall the non-perturbative uncertainties for beauty are significantly smaller than perturbative uncertainties.

3. Experimental methods

Beauty production is a small fraction of the total cross section at HERA: $\sigma_{b\bar{b}}/\sigma_{\rm tot} \sim 0.1\%$ which increases to $\sim 6\%$ for high-p_T jets and to $\sim 4\%$ in DIS at high-Q^2 and low x. This makes the measurement of beauty production quite difficult. Fortunately, beauty and charm decays are the main source of high-p_T leptons originating in the proximity of the interaction region. Therefore many analyses concentrated on leptonic tags. In a sample of events with two jets and a high-p_T lepton, a b fraction larger than 20% can be achieved.

The beauty content of a sample of events with jets and leptons can then be obtained by exploiting the transverse momentum of the lepton with respect to the associated jet axis, $p_T^{\rm rel}$, which is harder for beauty than for charm and light flavours (LF) due to the large B mass. In practice the $p_T^{\rm rel}$ distribution of the data is fitted with MC templates for b, c and LF to find the optimal b fraction (Fig. 2(b)). It is very important that realistic templates are used in these fits, possibly checked (and corrected if needed) using control samples of data.

When data from a precise vertex detector are available, the impact parameter of the lepton with respect to the interaction vertex in the transverse plane, δ, can be used to tag leptons originating from a displaced vertex due to a heavy hadron decay. A negative sign is assigned to δ if the lepton trajectory crossed the axis of the associated jet upstream of the event vertex, such that leptons from true secondary vertices have a tail at positive δ while tracks from the primary vertex have a symmetric δ distribution around zero due to resolution (Fig. 2(c)).

The H1 collaboration used a combination of δ and $p_T^{\rm rel}$ in all the measurements with a leptonic tag except for the first paper which used $p_T^{\rm rel}$ alone. Since ZEUS didn't have a silicon ver-
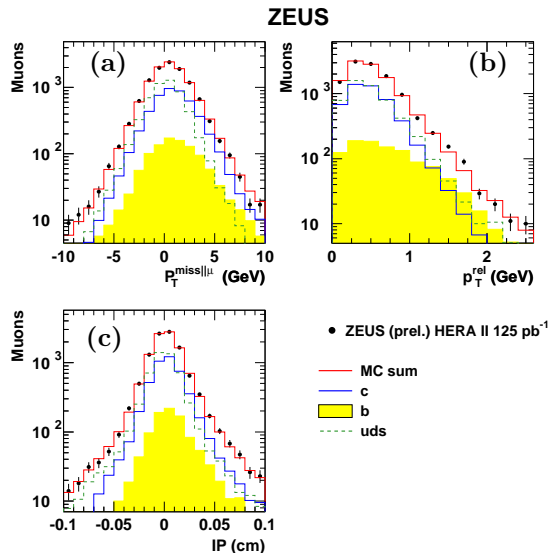

Figure 2. Distributions of discriminant variables used to extract the b and c content of the ZEUS muon DIS sample [13]: (a) $p_T^{{\rm miss}||\mu}$, (b) $p_T^{\rm rel}$ and (c) δ (here called IP). The points represent the data while the histograms are the b, c and light flavour (uds) MC templates normalised according to the fit results, and their sum.
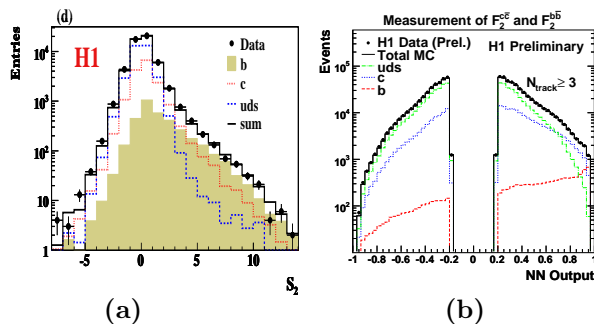

Figure 3. Variables used to extract the b and c content of inclusive samples: (a) S_2 for the H1 dijet sample [21] and (b) the neural network output from the H1 DIS analysis [14].

tex detector in the HERA I phase, all the ZEUS measurements based on HERA I data are based on $p_T^{\rm rel}$. ZEUS preliminary results from HERA

II data use a combination of δ and $p_T^{\rm rel}$ [12] or a combination of $p_T^{\rm rel}$, δ and the missing momentum in the muon direction $p_T^{{\rm miss}||\mu}$ [13] which is an indication of the presence of a neutrino from a semileptonic decay (Fig. 2(a)). This variable requires a hadronic calorimeter with very good and well understood resolution.

While δ and $p_T^{{\rm miss}||\mu}$ give a good separation between light and heavy flavours, $p_T^{\rm rel}$ has the best discriminating power between b and c plus LF.

The information from the silicon vertex detector can be further exploited to tag beauty in inclusive events, without the need of lepton requirements. The H1 collaboration developed an inclusive lifetime tagging technique based on the impact parameter of inclusive charged tracks. All the charged tracks in an event with ≥ 2 hits in the silicon tracker and $p_T > 0.5$ GeV are sorted according to their impact parameter significance $S = \delta/\sigma_\delta$ such that S_1 is the highest significance in absolute value, S_2 the second, etc. . In events with $S_1 S_2 > 0$, S_2 shows a positive tail dominated by beauty (Fig. 3(a)) which can be exploited, together with S_1, to extract the c and b content of the sample. In a recent preliminary result [14] this technique has been improved by feeding several track–based variables into a neural network. The network output is shown in Fig. 3(b).

4. Photoproduction results

4.1. Events with two jets

The first measurement of b production at HERA exploited events with two jets and a muon to obtain the total γp cross section [15]. The result was ~ 3 times larger than the NLO prediction, probably because of an unrealistic MC model used in the analysis. The early ZEUS result based on electron tagging [16] was not precise enough to be conclusive.

The precision and reliability of the beauty measurements improved significantly with the following generation of results on b production with two jets and a muon [17,18]. They were in general agreement with each other and with NLO predictions, the only exception being an excess of data over theory in the lowest p_T^μ bin observed in [18].

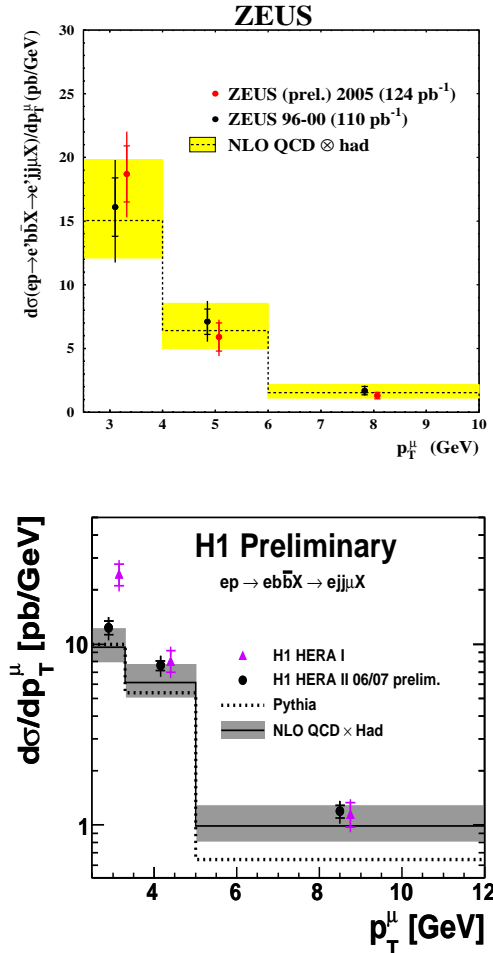Two preliminary results on b production in

Figure 4. Differential cross sections for beauty production with two jets ($p_T^{\rm j1, j2} > 7, 6$ GeV) and a muon as a function of the muon transverse momentum for $Q^2 < 1$ GeV^2 and $0.2 < y < 0.8$. The upper plot shows the ZEUS preliminary [12] and published [17] results for the pseudorapidity range $-1.6 < \eta^\mu < 2.3$. The lower plot shows H1 preliminary [19] and published [18] results for the pseudorapidity range $-0.55 < \eta^\mu < 1.1$. The measurements are compared to NLO QCD predictions.

events with two jets and a muon have been presented recently at conferences (Fig. 4). The first one is based on the first data collected with the

ZEUS microvertex detector [12]. This measurement, which uses a combination of δ and p_T^{rel}, confirms previous results obtained with p_T^{rel} alone. The second one by H1 is based on a large fraction of the HERA II luminosity [19]. The results are in good agreement with NLO QCD, within the NLO uncertainty band, and do not confirm the excess observed at low muon p_T in the previous H1 publication.

Recently, ZEUS published a measurement of beauty production in events with two jets and an electron [20]. Electrons from semileptonic beauty decays were tagged using a likelihood ratio method, based on calorimeter and tracking (dE/dx) information to select electrons, on p_T^{rel} and on the direction of the missing momentum. This method allows a lower lepton p_T threshold than that used for muons. As shown in Fig. 5, the electron results are also in good agreement with the NLO prediction.
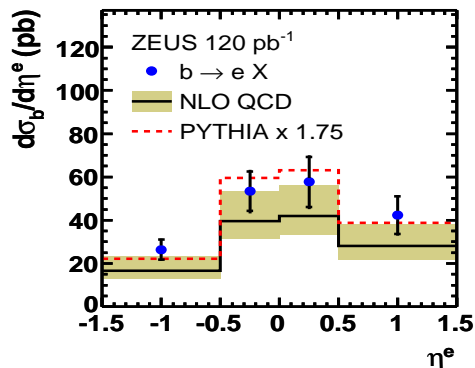

Figure 5. Differential cross section for beauty production with two jets ($p_T^{\text{jet}} > 7, 6$ GeV) and an electron as a function of the electron pseudorapidity for $p_T^e > 0.9$ GeV, $Q^2 < 1$ GeV^2 and $0.2 < y < 0.8$ as measured by ZEUS [20], compared to NLO QCD predictions.

The H1 collaboration used the inclusive lifetime tagging technique to measure the b and c content of a high-p_T ($p_T^{\text{j1,j2}} > 11, 8$ GeV) dijet sample [21]. The results are in agreement with NLO QCD and extend results from leptonic tags to higher jet p_T.

While the overall agreement of dijet measurements with NLO QCD is quite satisfactory, it is interesting to look at particular regions of the phase space where the theoretical description may be problematic. A possible candidate is the region of low x_γ^{jets} that is dominated by resolved-photon interactions and multi–jet topologies. Figure 6 shows the x_γ^{jets} distributions from all the beauty dijet measurements. The peak at $x_\gamma^{\text{jets}} = 1$, related to the BGF pro-

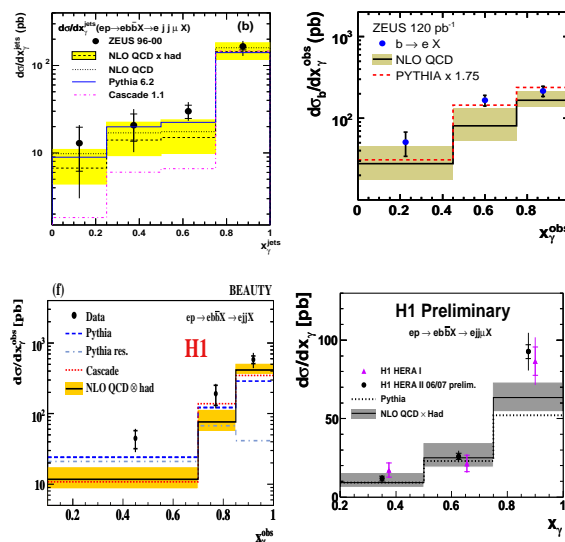Figure 6. Differential cross sections as a function of x_γ^{jets} for all HERA dijet measurements. Upper plots: ZEUS with muons [17] and electrons [20]. Lower plots: H1 inclusive [21] and muons [19]. All compared with NLO QCD.

cess, is apparent and reasonably well reproduced by NLO QCD. The description of the low x_γ^{jets} tail is also satisfactory, although with large uncertainties. Similar results have been obtained for $\Delta\Phi^{jj}$ [19].

4.2. Double tag analyses

The beauty fraction in a selected sample can be increased by requiring two b tags in the same event, i.e. two leptons or a lepton and a reconstructed D meson. The first double–tag analyses exploited $D^* - \mu$ correlations [22,23]. The

recent ZEUS analysis of dimuon events [24] produced significantly more precise results. A sample of events with two non-isolated muons with invariant mass $m_{\mu\mu} > 4$ GeV was selected. This sample originates mainly from B decays and from backgrounds from misidentified muons and from in-flight decays of πs and Ks. Since these backgrounds are charge-symmetric, they can be removed by subtracting the number of unlike-sign pairs, N^u, from the number of like-sign pairs, N^l. The resulting difference corresponds to the number of $b\bar{b}$ events, $N_{b\bar{b}}$, times the difference between the probability P^u for a $b\bar{b}$ pair to produce two unlike–sign muons ($b \to \mu^-, \bar{b} \to \mu^+$ +c.c.; ...) and the probability P^l for producing two like-sign muons ($b \to \mu^-, \bar{b} \to \bar{c} \to \mu^-$ + c.c.): $N^u - N^l = N_{b\bar{b}}(P^u - P^l)$. The small contribution from charm and vector meson decays in the unlike-sign sample and acceptance effects have been corrected for. The b cross sections measured with this method are in agreement with NLO QCD calculations (Fig. 7). Double tag
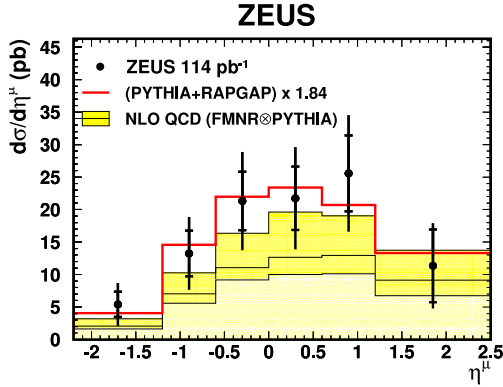

Figure 7. Differential cross section for muons from b decays in events with two muons with $p_T^\mu > 1.5$ GeV and $-2.2 < \eta^\mu < 2.5$ as a function of η^μ as measured by ZEUS [24], compared to NLO QCD predictions.

methods have significant acceptance for b quarks produced at very low p_T. The ZEUS dimuons analysis covers the full b quark phase space, with the exception of the region of very forward ra-

pidities, which is expected to contribute $\sim 10\%$ to the total cross section . This allowed the measurement of the total $b\bar{b}$ cross section:

$$\sigma_{\text{tot}}(ep \to b\bar{b}X) = 13.9 \pm 1.5(\text{stat.})^{+4.0}_{-4.3}(\text{syst.})\,\text{nb}$$

in agreement within uncertainties with the FMNR prediction

$$\sigma_{\text{tot}}^{\text{NLO}}(ep \to b\bar{b}X) = 7.5^{+4.5}_{-2.1}\,\text{nb}.$$

4.3. Summary

For a more direct comparison, cross sections obtained with different experimental techniques in different visible kinematic regions, $\sigma_{\text{vis}}^{\text{exp}}$, have been transformed into differential cross sections in the transverse momentum of the b quark, p_T^b, using the NLO theory:

$$\frac{d\sigma}{dp_T^b} = \sigma_{\text{vis}}^{\text{exp}} \times \frac{d\sigma^{\text{NLO}}/dp_T^b}{\sigma_{\text{vis}}^{\text{NLO}}}.$$

All the HERA results (but [15]) are shown in Fig. 8. The data obtained with different methods and in different kinematic regions are in good agreement among each other and with NLO QCD. The most precise data are from dijet–plus–muon results, which have a precision of $\sim 15\%$. The central value of the NLO QCD prediction shown in Figures 4-7, calculated with $\mu_r = \mu_f = m_T$, corresponds to the dotted line of Fig. 8. The full line and the uncertainty band of Fig. 8 have been calculated with $\mu_r = \mu_f = \frac{1}{2}m_T$ which was recently advocated as a better choice [25].

5. $F_2^{b\bar{b}}$ and b PDFs

5.1. $F_2^{b\bar{b}}$

The recent trend of beauty measurements in DIS is towards a determination of the beauty structure function $F_2^{b\bar{b}}$. Experimentally $F_2^{b\bar{b}}$, $F_L^{b\bar{b}}$ and the reduced cross section $\tilde{\sigma}^{b\bar{b}}$ are defined, in analogy to the inclusive case, from the double differential $b\bar{b}$ cross section in x and Q^2:

$$\frac{d^2\sigma^{b\bar{b}}}{dxdQ^2} = (\hbar c)^2 \frac{2\pi\alpha_{em}^2}{xQ^4}\, Y_+ \, \tilde{\sigma}^{b\bar{b}}(x, Q^2, s)$$

$$\tilde{\sigma}^{b\bar{b}}(x, Q^2, s) = F_2^{b\bar{b}}(x, Q^2) - \frac{y^2}{Y_+}F_L^{b\bar{b}}(x, Q^2)\,,$$
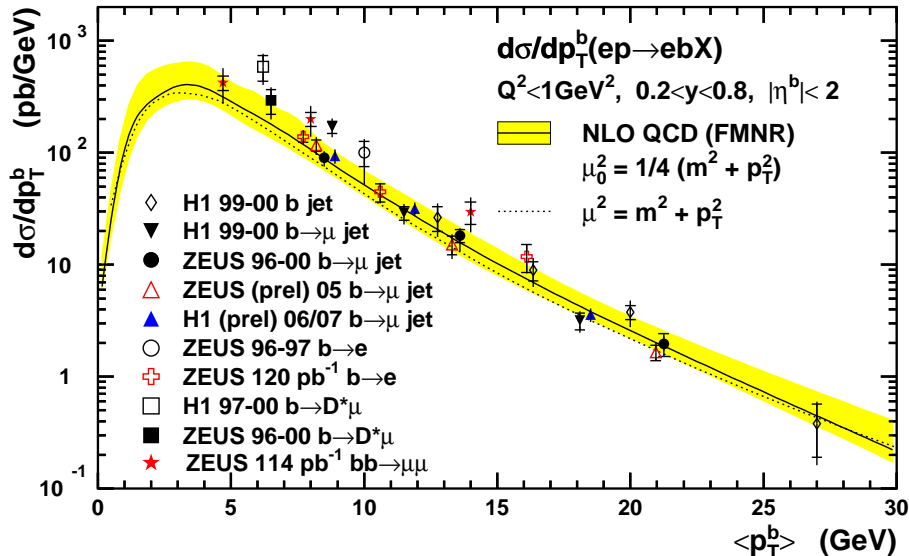
HERA

Figure 8. Differential cross sections as a function of the p_T of the b quark extracted from all the HERA measurements of beauty photoproduction. The references, corresponding to the symbol keys, are from top to bottom: [21,18,17,12,19,16,20,22–24].

where $Y_+ = 1 + (1-y)^2$, $y = Q^2/xs$. It should be noted that this definition does not correspond to that used in some theoretical works [7,26]. In particular, it has the problem of not being an infrared safe quantity.

There are advantages and disadvantages in measuring $F_2^{b\bar{b}}$ rather than cross sections for specific final states (i.e. leptons and/or jets in a given phase space). The main advantage is that $F_2^{b\bar{b}}$ is more fundamental, i.e. simpler to calculate by theorists, and it does not need non–perturbative corrections for HQ fragmentation and decay, and for jet hadronisation. Indeed, calculations using different theoretical approaches [7,26] are available for $F_2^{b\bar{b}}$ but not for specific final state observables. The main disadvantage is that detectors are sensitive mainly to central production at high–p_T, and therefore a measurement of the full phase space may introduce some model-dependent extrapolation. This is not a serious problem for beauty as it is for charm. The whole b quark phase space can in fact be accessed ex-

perimentally. As an example, Fig. 9 shows the fraction $\mathcal{A}$ of muons produced in b or $\bar{b}$ decays covered by the visible kinematic region of [13] ($p_T^\mu > 1.5$ GeV, $-1.6 < \eta^\mu < 2.3$). $\mathcal{A}$ ranges from 18% to 40% as the p_T of the b quark goes from zero to 15 GeV, and varies between 28% at central b rapidities to $\sim 10\%$ at very forward rapidity.

5.2. The beauty PDF

The QCD calculations discussed so far are often referred to as calculations in the fixed flavour number scheme (FFNS), in the sense that only light flavours are active in the proton PDFs and HQs are generated in the hard interaction. Another approach, historically used in PDF analyses, is the variable flavour number scheme (VFNS) in which HQs are treated as massless partons in the proton above some minimal threshold (e.g. for $Q^2 > m_Q^2$), with a corresponding non-zero PDF. In the simplest version of this approach, the zero-mass VFNS (ZM-VFNS), at leading order, the HQ structure function $F_2^{q\bar{q}}$ is simply obtained from the heavy quark PDF,
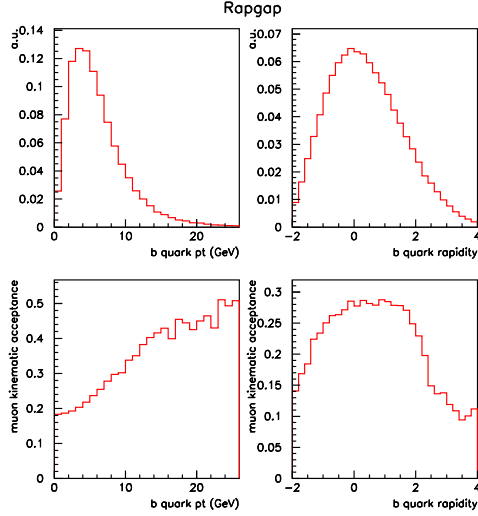
Figure 9. Upper plots: the distribution of the b quarks transverse momentum, p_T^b, (left) and rapidity, Y^b, (right) according to the Rapgap MC for $Q^2 > 20 \, \mathrm{GeV}^2$. Lower plots: the fraction $\mathcal{A}$ of muons in the ZEUS visible kinematic region [13] as a function of p_T^b (left) and Y^b (right).

$f_q(x, Q^2)$, as: $F_2^{q\bar{q}} = 2e_q^2 x f_q(x, Q^2)$. This approach is valid only for $Q^2 \gg m_q^2$, well outside the range of beauty measurements at HERA, as it does not include properly mass effects.

Anyway, the concept of HQ PDFs is quite useful: it can include naturally an intrinsic HQ component in the proton as proposed by Brodsky et al. [27], it provides an effective resummation of large logarithms of Q^2/m_q^2, and it provides a basic ingredient for the calculations of HQ–initiated processes at hadron colliders (e.g. $b\bar{b} \to H$).

For these reasons improved versions of the VFNS (GM-VFNS) [7] have been developed recently, matching the FFNS results at low Q^2 and the ZM-VFNS results at high Q^2. As these schemes are currently used in global PDF fits, it is important to check that they can reproduce charm and beauty data from HERA.

In another approach, HQ PDFs valid for $Q^2 \gg m_q^2$ (e.g. for hadron colliders) are obtained starting from a FFNS analysis of HERA data [28].
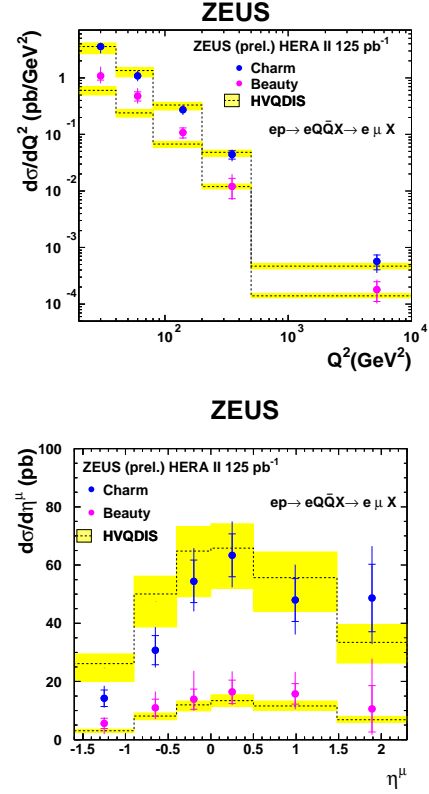

Figure 10. Differential cross sections for muons from charm and beauty decays as a function of Q^2 (up) and η^μ (down), for $p_T^\mu > 1.5 \, \mathrm{GeV}$, $-1.6 < \eta^\mu < 2.3$, $Q^2 > 20 \, \mathrm{GeV}^2$ and $0.01 < y < 0.7$ [13].

6. DIS results

6.1. Leptonic tag analyses

Experimentally, DIS events are defined by the presence of the scattered electron in the detector. This corresponds roughly to $Q^2 > 1 \, \mathrm{GeV}^2$ at HERA I and $Q^2 > 4 \, \mathrm{GeV}^2$ at HERA II.

The first studies [29,18] of b production in DIS measured the cross section for events with a muon and a jet in the Breit frame. The request of a jet in the Breit frame was used to suppress processes of order zero in α_s ($\gamma^* q \to q'$) with respect to higher–order processes such as heavy quark production from BGF ($\gamma^* g \to b\bar{b}$). The p_T^{rel} method was used to extract the beauty fractions, in combination with δ in the H1 case. The results were

in agreement with the HVQDIS calculation for $Q^2 \gtrsim 10$ GeV^2 and about two standard deviations above the calculation at lower Q^2.

The first ZEUS preliminary result on $F_2^{b\bar{b}}$ used the first 39 pb^{-1} of HERA II data collected in 2003-04. It was based on the measurement of events with a muon and an associated jet in the laboratory frame and on the $p_T^{\rm rel}$ method [30].

More recent preliminary results [13] from ZEUS used 125 pb^{-1} of data collected in 2005 to measure simultaneously charm and beauty in events with a muon at $Q^2 > 20$ GeV^2 (Fig. 2). The cross sections for charm and beauty as a function of Q^2 and η^μ are shown in Fig. 10.

6.2. Inclusive analyses and $F_2^{b\bar{b}}$

H1 used the inclusive tagging technique to measure the c and b content of inclusive DIS events in order to extract $F_2^{b\bar{b}}$. The first results were based on HERA I data [31]. They have been combined recently with preliminary results based on the almost full HERA II luminosity [14]. These combined HERA I+II results are the most precise measurements of b production in DIS available, with total uncertainties of $\sim 20\%$ at intermediate Q^2. Figure 11 shows the $F_2^{b\bar{b}}$ data from the two preliminary ZEUS muon analyses and from the H1 combined HERA I+II inclusive data. The charm results are well reproduced by HVQDIS. Beauty cross sections are somewhat higher than HVQDIS at low Q^2 but still compatible. These data were also used to extract $F_2^{b\bar{b}}$. The first ZEUS preliminary results lie above the H1 data, while the more recent ZEUS points are in between the two. Considering that systematics are largely correlated, the overall agreement is acceptable. The figure also shows NLO QCD calculations in the FFNS (labelled CTEQ5F) and calculations in the GM-VFNS (MRSTW08 and CTEQ6.6). An improvement in the precision of the data would be needed to be able to distinguish between different theoretical approaches.

7. Conclusions and perspectives

A wealth of beauty photoproduction measurements is now available at HERA, they have been obtained with different experimental techniques
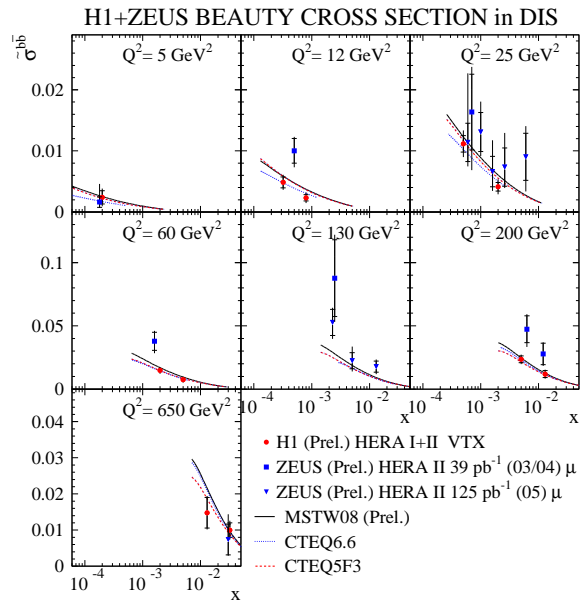

Figure 11. Reduced cross section $\tilde{\sigma}^{b\bar{b}}$ as a function of x at different values of Q^2. The circles are a combination of HERA I and preliminary HERA II results from H1 [14], the squares [30] and the triangles [13] are ZEUS preliminary results from two different HERA II data sets. The curves represent QCD calculations at NLO in the FFNS (CTEQ5F3) and in two versions of the GM-VFNS (MSTW08 and CTEQ6.6) [26].

and cover a wide kinematic range, from the total cross section to high p_T jets. In many cases the precision is at the $15 - 20\%$ level, considerably smaller than the theoretical uncertainty. The agreement between NLO QCD and the experimental data is good. Possible discrepancies suggested by early results have been ruled out.

Impressive progress has also been achieved in DIS. $F_2^{b\bar{b}}$ has been measured at several x and Q^2 points and with uncertainties as small as $\sim 20\%$. Some differences at the two standard deviations level between the muon–based analyses and the HVQDIS prediction deserve some further investigations. The experimental uncertainties in DIS are still larger than the theoretical ones, but there is well motivated hope for improvement in the

next years. The systematic errors of the H1 data can be further reduced, and ZEUS results based on inclusive lifetime tags and on the full HERA luminosity are still to come. Finally, improvements are expected from the combination of b and c data from the two collaborations.

I wish to thank the organizing committee and the MPI for the fruitful days spent talking about physics in Schloss Ringberg.

REFERENCES

1. S. Frixione *et al.*, Phys. Lett. B **319** (1993) 339.
2. S. Frixione *et al.*, Nucl. Phys. B **412** (1994) 225.
3. B.W. Harris and J. Smith, Nucl. Phys. B **452** (1995) 109; B.W. Harris and J. Smith, Phys. Lett. B **353** (1995) 535, Erratum-ibid. B **359** (1995) 423.
4. E. Norrbin and T. Sjöstrand, Eur. Phys. J. C **17** (2000) 137.
5. O. Behnke *et al.*, *Benchmark cross sections for heavy flavour production*, proceedings of the workshop "HERA and the LHC 2004-2005" p.405, hep-ph/0601013.
6. M. Cacciari *et al.*, JHEP **03** (2001) 006; G. Kramer and H. Spiesberger, Eur. Phys. J. C **38** (2004) 309.
7. A. Chuvakin *et al.*, Phys. Rev. D **62** (2000) 036004; R.S. Thorne and W.K. Tung, to appear in the proceedings of the workshop "HERA and the LHC 2007/2008", arXiv:0809.0714 [hep-ph].
8. A.V. Lipatov and N.P. Zotov, Phys. Rev. D **73** (2006) 114018; A.V. Lipatov and N.P. Zotov, JHEP **0608** (2006) 043.
9. R. Bonciani *et al.*, Nucl. Phys. B **529** (1998) 424, Erratum-ibid. B **803** (2008) 234.
10. T. Carli *et al.*, JHEP **09** (2003) 070.
11. M. Cacciari *et al.*, JHEP **0604** (2006) 006; J. Braciník et al., *Heavy quark fragmentation*, proceedings of the workshop "HERA and the LHC 2004-2005" p.390, hep-ph/0601013.
12. ZEUS Collaboration, *Measurement of beauty photoproduction at HERA II*, presented at EPS-HEP07, ZEUS-prel-07-020.
13. ZEUS Collaboration, *Charm and beauty in DIS from muons*, presented at ICHEP08, ZEUS-prel-08-007.
14. H1 Collaboration, *Measurement of F_2^{cc} and F_2^{bb} using the H1 vertex Detector at HERA*, presented at ICHEP08, H1prelim-08-173.
15. C. Adloff *et al.* [H1 Collaboration], Phys. Lett. B **467** (1999) 156, Erratum-ibid. B **518** (2001) 331.
16. J. Breitweg *et al.* [ZEUS Collaboration], Eur. Phys. J. C **18** (2001) 625.
17. S. Chekanov *et al.* [ZEUS Collaboration], Phys. Rev. D **70** (2004) 012008, Erratum-ibid. D **74** (2006) 059906.
18. A. Aktas *et al.* [H1 Collaboration], Eur. Phys. J. C **41** (2005) 453.
19. H1 Collaboration, *Beauty using events with a muon and jet in photoproduction*, presented at ICHEP08, H1prelim-08-071.
20. S. Chekanov *et al.* [ZEUS Collaboration], Phys. Rev. D **78** (2008) 072001.
21. A. Aktas *et al.* [H1 Collaboration], Eur. Phys. J. C **47** (2006) 597.
22. A. Aktas *et al.* [H1 Collaboration], Phys. Lett. B **621** (2005) 56.
23. S. Chekanov *et al.* [ZEUS Collaboration], Eur. Phys. J. C **50** (2007) 299.
24. S. Chekanov *et al.* [ZEUS Collaboration], submitted to JHEP, preprint DESY-08-129.
25. A. Geiser, arXiv:0711.1983 [hep-ex], DIS07 proceedings, http://dx.doi.org/10.3360/dis.2007.163.
26. W.K. Tung *et al.*, JHEP **0702** (2007) 053; A.D. Martin *et al.*, Phys. Lett. B **652** (2007) 292.
27. S.J. Brodsky *et al.*, Phys. Lett. B **93** (1980) 451.
28. M. Glück *et al.*, Phys. Lett. B **664** (2008) 133.
29. S. Chekanov *et al.* [ZEUS Collaboration], Phys. Lett. B **599** (2004) 173.
30. ZEUS Collaboration, F_2^b *at HERA II*, presented at DIS07, ZEUS-prel-07-007; B. Kahle, DIS07 proceedings, http://dx.doi.org/10.3360/dis.2007.164.
31. A. Aktas *et al.* [H1 Collaboration], Eur. Phys. J. C **40** (2005) 349; A. Aktas *et al.* [H1 Collaboration], Eur. Phys. J. C **45** (2006) 23.